Journal of Imaging Informatics in Medicine (2025) 38:1904–1913
https://doi.org/10.1007/s10278-024-01291-8

ORIGINAL PAPER

A Machine Learning Model Based on Global Mammographic Radiomic Features Can Predict Which Normal Mammographic Cases Radiology Trainees Find Most Difficult

Somphone Siviengphanom[1] · Patrick C. Brennan[1] · Sarah J. Lewis[1,2] · Phuong Dung Trieu[1] · Ziba Gandomkar[1]

Received: 1 June 2024 / Revised: 28 September 2024 / Accepted: 30 September 2024 / Published online: 15 October 2024

Abstract

This study aims to investigate whether global mammographic radiomic features (GMRFs) can distinguish *hardest-* from *easiest-to-interpret* normal cases for radiology trainees (RTs). Data from 137 RTs were analysed, with each interpreting seven educational self-assessment test sets comprising 60 cases (40 normal and 20 cancer). The study only examined normal cases. Difficulty scores were computed based on the percentage of readers who incorrectly classified each case, leading to their classification as *hardest-* or *easiest-to-interpret* based on whether their difficulty scores fell within and above the 75th or within and below the 25th percentile, respectively (resulted in 140 cases in total used). Fifty-nine *low-density* and 81 *high-density* cases were identified. Thirty-four GMRFs were extracted for each case. A random forest machine learning model was trained to differentiate between *hardest-* and *easiest-to-interpret* normal cases and validated using leave-one-out-cross-validation approach. The model's performance was evaluated using the area under receiver operating characteristic curve (AUC). Significant features were identified through feature importance analysis. Difference between *hardest-* and *easiest-to-interpret* cases among 34 GMRFs and in difficulty level between *low-* and *high-density* cases was tested using Kruskal–Wallis. The model achieved AUC = 0.75 with *cluster prominence* and *range* emerging as the most useful features. Fifteen GMRFs differed significantly ($p < 0.05$) between *hardest-* and *easiest-to-interpret* cases. Difficulty level among *low-* vs *high-density* cases did not differ significantly ($p = 0.12$). GMRFs can predict *hardest-to-interpret* normal cases for RTs, underscoring the importance of GMRFs in identifying the most difficult normal cases for RTs and facilitating customised training programmes tailored to trainees' learning needs.

Keywords Radiomics · Mammography · Difficult normal cases · Radiology trainees · Machine learning · Gist

Abbreviations

AUC	Area under receiver operating characteristic curves
BC	Breast cancer
BI-RADS	Breast imaging and reporting data system
BREAST	Breastscreen REader Assessment STrategy
CC	Craniocaudal
FOS	First-order statistics
GLCM	Gray level co-occurrence matrix
GMRFs	Global mammographic radiomic features
MLO	Mediolateral oblique
NGTDM	Neighbourhood gray-tone difference matrix
RANZCR	Royal Australian and New Zealand College of Radiologists
ROI	Multiple regions of interests defined by the lattice-based approach covering the entire breast image
RTs	Radiology trainees
SQ	Largest square rectangular box inscribed within breast

✉ Somphone Siviengphanom
ssiv6387@uni.sydney.edu.au

[1] Medical Image Optimisation and Perception Group, Discipline of Medical Imaging Science, Faculty of Medicine and Health, Sydney School of Health Sciences, Susan Wakil Health Building D18, the University of Sydney, Sydney, NSW 2006, Australia

[2] School of Health Sciences, Western Sydney University, Sydney, NSW 2751, Australia

Introduction

Female breast cancer (BC) stands as one of the leading causes of cancer-related mortality worldwide [1]. Mammographic screening programmes, aimed at early detection of BC, have been shown to significantly reduce BC mortality rate by up to 40% [2]. However, interpreting mammograms is a challenging task susceptible to errors, and relying primarily on technological advancements is insufficient to mitigate or address these challenges [3]. Previous studies have reported that correctly interpreting normal cancer-free mammograms can also be highly difficult for readers with inadequate mammographic reading experience such as radiology trainees (RTs) [4, 5]. The capability of readers including RTs to accurately interpret screening mammograms plays a pivotal role in the efficacy of breast screening programmes. Despite efforts to propose criteria for screen reader certification aimed at reducing diagnostic variability among readers, none of the current guidelines for these criteria serve as strong predictors of reader performance [6, 7]. As a result, wide inter-reader variability persists, highlighting the critical need to prioritise education and training for readers, especially for less experienced readers like RTs, in this domain [6–9]. Given that normal cases comprise over 99% of all cases in breast screening programmes [10, 11], along with the fact that false-positive screening results cause huge healthcare costs of nearly US$3 billion yearly (in the USA as an example) and psychological distress to patients due to unnecessary recalls involving invasive procedures [12], it is imperative that education strategies are prioritised to give extra attention to normal cases.

Studies from medical image perception and basic vision science demonstrate that exposing RTs to large mammographic normal cases via test set training programmes, often containing nearly 70% of normal cases in a test set, can enhance their expertise development in interpreting normal cases [13–15]. Still, the present test set curation process using experts' or individual's perception of case difficulty via the breast imaging and reporting data system (BI-RADS) breast density and/or benign features are unreliable predictors of normal cases' difficulty among RTs [11, 16–18]. Therefore, there is a strong demand for a more systematic approach of predicting RTs' difficult normal cases so that customised mammographic training test sets for RTs can be facilitated while their false positive errors can be better monitored and improved.

The process of interpreting medical images necessitates the development of capabilities for globally processing images. Earlier studies showed that individuals with less experience such as RTs often lack the ability to swiftly process the global clues indicative of abnormalities [19]. To investigate this further, we designed an experiment protocol to gather the initial impressions of radiologists regarding the abnormality of a case, known as the gist signal [19–21]. This signal not only indicates a current cancer case [22] but also serves as a predictor of future BC [21]. Moreover, recent research in radiomics has shown that quantitative global mammographic radiomic (or computer extract image) features align closely with the holistic perceptual information gleaned from radiologists' rapid first impressions about the presence of an image abnormality or global gist signal [20, 23]. This signal has proven valuable in guiding visual searches and aiding in making diagnostic decisions when interpreting challenging mammographic cases [11, 22, 24].

Radiomic features capture various aspects of the mammogram, including texture, intensity, and spatial relationships, providing comprehensive information about the underlying tissue characteristics [25, 26]. Radiomic features have been the subject of systematic investigation in previous works, where local radiomic features were utilised to identify missed mammographic masses and false positive location errors of RTs, achieving area under receiver operating characteristic curves (AUCs) from 0.59 to 0.61 and accuracies from 12 to 40%, respectively [4, 5]. More recent studies [11, 16] have revealed that using global mammographic radiomic features (GMRFs), the most difficult/easiest normal cases for readers in general and experienced radiologists can be accurately predicted (AUCs of up to 0.73). However, to date, there has been no study exploring whether GMRFs can specifically predict *hardest-* from *easiest-to-interpret* normal cases for RTs. Considering the fact that RTs are still developing their holistic processing capabilities compared to experienced radiologists [13, 21, 22, 24], this paper explores whether GMRFs can serve as reliable predictors specifically for *hardest-to-interpret* normal cases for RTs. It also seeks to recognise if there are any specific significant GMRFs that denote the *hardest-to-interpret* normal cases for RTs. Knowing these could be valuable not only in the training programs' test set curation process of most difficult normal cases for RTs but also facilitating their expertise development in recognising normal image features that could be most difficult for them often resulting in false positive errors. This is so that their specific skills in perceiving the global signature of normality can be well developed since RTs are generally not as good at recognising the normal features as compared to experienced radiologists [13, 24, 27].

Furthermore, since the current approach to curating test sets relies on experts' opinions regarding case difficulty, primarily using breast density as a surrogate metric [11, 16–18], we also examine if a significant difference exists in difficulty level between *low-density* (BI-RADS category A = fatty and B = fibroglandular) and *high-density* (category C = heterogeneous and D = extremely dense) normal cases.

Materials and Methods

Readers

Ethical approvals of this research were acquired from the University of Sydney's Human Research Ethics Committee [protocol no. 2019/013 and 2017/028], which included obtained written informed consent from each reader participating in the study.

A total of 137 Australian and New Zealand RTs who participated in the BREAST (Breastscreen REader Assessment STrategy) programme [28] from 04 September 2014 to 23 February 2021 were included in the study. The mean age of the readers was 33 based on the age details provided by 116 RTs, while 21 did not provide their age details. In total, 19% of the readers engaged in the programme through a radiology/BC conference/workshop in a simulated reading room, while 81% completed the programme online through the BREAST platform (https://breast-australia.sydney.edu.au/) at their usual clinical workplace. Reading conditions in both settings were equivalent with cases being presented on two 5-megapixel medical standard monitors including ambient light levels range of 20–40 lx [29]. RTs generally had less than 1 year experience reading mammograms (59%), read less than 20 mammographic cases per week (79%), and spent less than 4 hour per week reading mammograms (96%). Also, 16 readers (12%) completed a fellowship in breast imaging that lasted for 3 to 6 months and had any experience reading images for a national breast screening programme (Table 1).

Table 1 Characteristics of readers ($n = 137$)

Mean years of age (derived from 116 radiology trainees' age details while 21 radiology trainees did not provide their age details)	33	
	N	**%**
Country		
Australia	135	99
New Zealand	2	1
Location at the time of engaging with the BREAST programme		
At a workshop or conference	26	19
At a clinic	111	81
# of years reading mammograms		
Less than 1	81	59
1 to 5	53	39
6 to 12	3	2
# of mammographic cases reading per week		
Less than 20	108	79
20 to 200	28	20
More than 200	1	1
# of hours per week spent reading mammograms		
Less than 4	131	96
4 to 30	5	4
More than 30	1	1
# of readers completed a fellowship lasted for 3 to 6 months		
Completed fellowship	16	12
Did not complete fellowship	119	87
Not specified	2	1
# of readers read for breast screening programme		
Yes	16	12
No	121	88

Mammographic Normal Cases

This retrospective study includes data from readers that completed seven BREAST test sets, each comprising 60 de-identified full-field digital mammographic (FFDM) cases, with 40 cases being cancer-free and 20 cases indicating cancer. For the purpose of this investigation, only normal cancer-free cases were included. Thus, a total of 280 normal FFDM cases (comprised of four images per case: two bilateral craniocaudal/CC and two mediolateral oblique/MLO views) acquired from screening asymptomatic women aged between 40 and 75 (mean and median = 57, standard deviation = 7, and range = 33 based on the age details of 130 women/cases, while ages of 10 women were not available due to anonymisation process) were utilised. These cases were collected from various mammography machines, including Fujifilm (Fujifilm Corporation, Minato City, Tokyo, Japan), GE (GE Healthcare, Chicago, IL, USA), Hologic (Hologic, Inc., Marlborough, MA, USA), Philips (Philips Healthcare, Amsterdam, the Netherlands), Sectra (Sectra, Linköping, Sweden), and Siemens (Munich, Germany). Each normal case's ground truth underwent confirmation of cancer-free status by at least two independent expert radiologists, each possessed over 20 years of experience, with validation through subsequent negative screen outcomes.

Categorising Hardest- vs Easiest-to-Interpret Normal Cases

To categorise normal cases as *hardest*- vs *easiest-to-interpret*, we initially calculated difficulty scores for each of the 280 normal cases using the Royal Australian and New Zealand College of Radiologists (RANZCR) scoring system [28] provided by the 137 RTs. A RANZCR score of 1 represents a normal case, while a score of 2 indicates that RTs considered the case as benign. Scores of 3, 4, or 5 signify an equivocal or malignant finding observed by the readers with higher numbers indicating a greater confidence of disease presence. Difficulty scores were computed by dividing the number of RTs who misclassified a normal case as cancer (provided a rating of 3, 4, or 5) by the total number RTs who read the test set. Subsequently, the 280 normal cases were then classified as *hardest*- and *easiest-to-interpret* cases based on the 75th and 25th percentiles of the cases containing the highest and lowest difficulty scores, correspondingly. This resulted in 70 *hardest*- and 70 *easiest-to-interpret* normal cases, totalling of 140 normal cases/560 DICOM images combined. To ensure a clear distinction between the most and least difficult normal cases in order to enable optimal feature learning for our machine learning model, only images in the upper and lower quartiles were used for further analysis. Normal cases in these two categories also resulted in a total of 59 *low-density* (35 *hardest*- and 24 *easiest-to-interpret*) and 81 *high-density* normal cases (35 *hardest*- and 46 *easiest-to-interpret*).

Global Radiomic Feature/Score Per Case

To obtain a global radiomic feature/score for each of the 140 normal cases, a total of 34 quantitative GMRFs of 560 images belonging to 140 cases extracted from the previous study [11] were used. Details about the GMRFs extraction method can be found in the previous study [11]. Briefly, from the 560 DICOM images, we first generated 560 binary masks using a standardised gray level threshold value set at 100 (manual adjustments on the value were also performed where needed) to extract the required breast region from its background while eliminating unwanted artefacts and labels. After that, we converted the DICOM images and masks to a TIFF file format, flipped all the right CC and MLO images to the left to have a consistent left-side chest wall on all images, and cropped the TIFF images and masks based on the maximum size of breast region. These cropped TIFF images and masks were used as input for the radiomic analysis (Fig. 1). We then outlined the region of interest on the images using the lattice-based/ROI (multiple regions of interests covering the entire breast image) [30] and squared-based/SQ (largest square rectangular box inscribed within

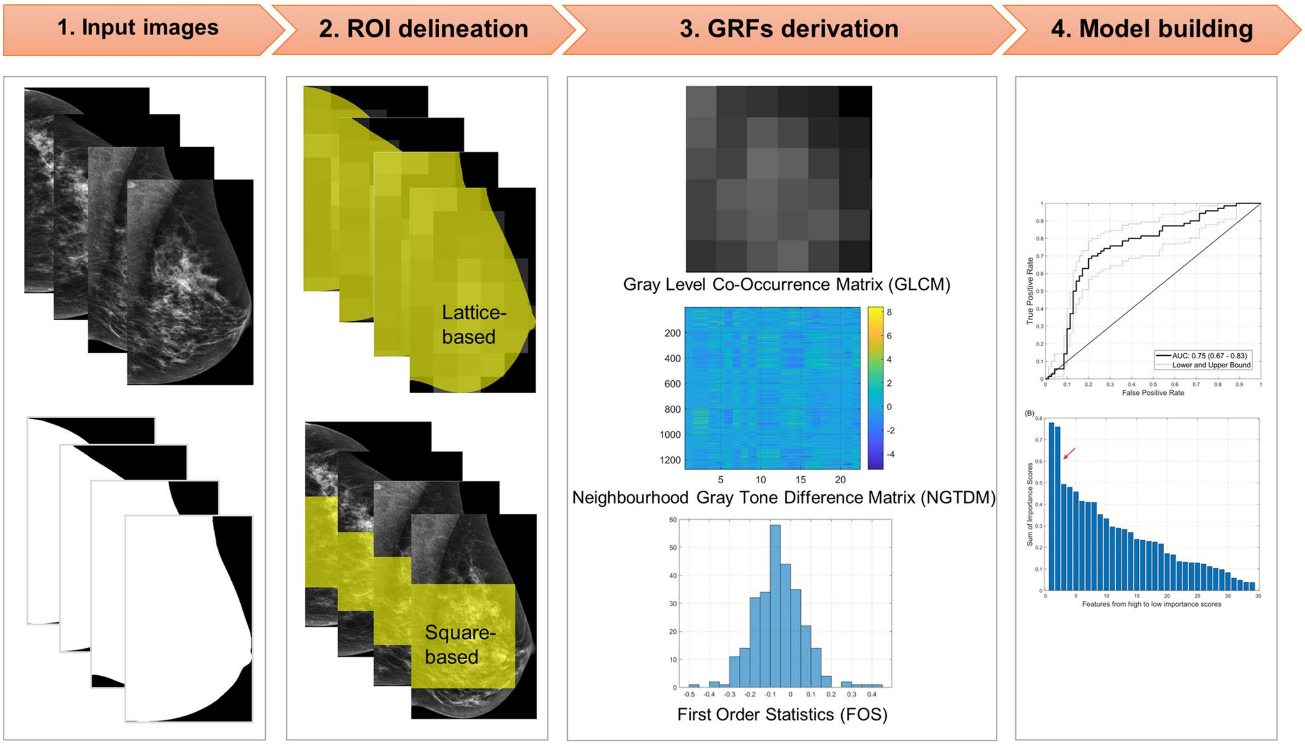

Fig. 1 Radiomics workflow. **1.** Input mammographic images and masks were acquired. **2.** Region of interest (yellow colour region) was delineated using lattice- and squared-based approaches. **3.** A set of 34 global mammographic radiomic features (GMRFs)/scores per image were extracted from the yellow region of interest, then standardised to have image intensity mean equal to zero and standard deviation equal to one. The extracted GMRFs of four images belonging to each of the 140 cases were then averaged to obtain one GMRF per case. **4.** Finally, using the averaged GMRFs, a random forest machine learning model for differentiating radiology trainees' *hardest*- from *easiest-to-interpret* normal cases was constructed and assessed

breast) [31] approaches. The 34 handcrafted GMRFs/scores per image were afterward extracted based on the region of interest delineated using our in-house MATLAB platforms and then normalised to calibrate image intensity mean to zero and standard deviation to one using a common z-score normalisation method [32]. Features using the ROI approach [30] were analysed using MATLAB distinct block processing technique (block size 214 × 214 pixels) and summarised using the standard deviation method. The extracted GMRFs of 4 images (i.e. 2 CC and 2 MLO images) belonging to a case were then combined and averaged to obtain one global radiomic feature/score per case.

The 34 GMRFs consisted of 30 Gray level co-occurrence matrix/GLCM-based Haralick texture features [33], 2 neighbourhood gray tone difference matrix/NGTDM-based texture features [34], and 2 first-order statistics/FOS-based features [25] (Table 2 and Fig. 1). These features were chosen because of their usefulness in describing mammographic appearances in measuring the contrast values of spatial inter-relationships between neighbouring pixels (GLCM and NGTDM) and the distribution of single pixel intensity value within the image region of interest (FOS) [25, 33].

Model Building

For the task of differentiating between normal cases that are *hardest-* and those of *easiest-to-interpret* for RTs, a random forest machine learning model was built using the averaged 34 GMRFs feeding through MATLAB ensemble of decision trees boosted with the adaptive logistic regression method (i.e. LogitBoost). The random forest with boosting approach was chosen due to its ability to produce an explainable model with automatic estimation of feature importance and its built-in feature selection approach which could minimise feature overfitting and potential selection bias problems [35]. Important GMRFs were recognised based on the analysis of feature importance scores using MATLAB's predictor importance algorithm, which also helps in identifying and mitigating redundant and biased features. Feature importance scores indicate how significant each feature was in the dataset when building the predictive model with larger value means larger effect the features had on the model in predicting *hardest-* from *easiest-to-interpret* normal cases of RTs (Fig. 1).

Statistical Analysis and Validation

In order to examine the performance of the model on our data and to maximise the use of the available data for both training and validation, we trained and validated the model using the resampling leave-one-out-cross-validation (LOOCV) approach (an unbiased, dependable, and accurate validation method for assessing a machine learning model' generalisation performance) [36]. Each time when training the model, all cases were used, except one case which was left out and used once as a test set to validate the model's predictive performance. We repeated this process 140 times (as per the total number of the normal cases we had) until each case was left out and used once as a test set. The model's performance was then evaluated based on how accurately it predicted the left-out/unseen case in each repetition, providing an effectively estimation of how well the model generalises to the unseen cases. The overall performance of the model for discriminating *hardest-* from *easiest-to-interpret* normal cases of RTs was assessed using the AUC.

A Kruskal–Wallis test was employed to investigate if the 34 GMRFs differed between *hardest-* and *easiest-to-interpret* normal cases of RTs, and if difficulty level differed among *low-* vs *high-density* normal cases of RTs. A p-value of less than 0.05 was considered statistically significant.

Moreover, a scree test of exploratory factor analysis [37] was used to determine the usefulness of the GMRFs based on the sum of their importance scores from the model.

Radiomics and statistical analysis were performed using MATLAB R2022a (MathWorks, Natick, MA, USA).

Results

Global Mammographic Radiomic Features Predicting Difficult Normal Cases of Radiology Trainees

The overall performance of the machine learning classification model for differentiating *hardest-* from *easiest-to-interpret* normal cases of RTs using GMRFs is shown in Fig. 2, which indicates an AUC of 0.75 (95% confidence interval, 0.67–0.83).

Significant Global Mammographic Radiomic Features and Breast Density of Difficult Normal Cases

Table 2 shows that 15 out of the total 34 GMRFs had a statistically significant difference between *hardest-* vs *easiest-to-interpret* normal cases of RTs with $p < 0.05$.

Table 2 and Fig. 3 show the significant GMRFs based on their importance scores derived from the predictive machine learning model. Out of the 34 features, when comparing each feature's total importance scores ranking from the highest to the lowest, two important features were recognised. These features were *SQ_Cluster_prominence_9* (feature# 31) of GLCM, and *ROI_Std_Range_all* (feature# 16)

Table 2 Extracted global mammographic radiomic features ($n = 34$)

Feature no.	Feature name	*p*-value	Feature importance score	Feature category	Parameters
1	ROI_Std_Correlation_3	0.207	0.229	GLCM	3-pixel distance between the pixel of interest and its neighbour
2	ROI_Std_Difference_entropy_3	0.775	0.104		
3	ROI_Std_Dissimilarity_3	0.218	0.134		
4	ROI_Std_Difference_variance_3	0.688	0.166		
5	ROI_Std_Energy_3	0.475	0.038		
6	ROI_Std_Entropy_3	0.621	0.112		
7	ROI_Std_Homogeneity_3	0.209	0.238		
8	ROI_Std_Information_measure_of_correlation1_3	0.654	0.129		
9	ROI_Std_Information_measure_of_correlation2_3	0.663	0.234		
10	ROI_Std_Maximum_probability_3	0.462	0.217		
11	ROI_Std_Sum_entropy_3	0.086	0.410		
12	ROI_Std_Sum_variance_3	0.558	0.039		
13	ROI_Std_Coarseness_3	0.869	0.409	NGTDM	3x3 neighbourhood size
14	ROI_Std_Cluster_prominence_3	0.756	0.493	GLCM	3-pixel distance between the pixel of interest and its neighbour
15	ROI_Std_Cluster_shade_3	0.905	0.353		
16	ROI_Std_Range_all	0.003^	0.759*	FOS	n/a
17	ROI_Std_Sum_of_squares_variance_9	0.555	0.225	GLCM	9-pixel distance between the pixel of interest and its neighbour
18	SQ_Correlation_9	0.028^	0.132		
19	SQ_Difference_entropy_9	0.000^	0.083		
20	SQ_Dissimilarity_9	0.000^	0.290		
21	SQ_Difference_variance_9	0.000^	0.128		
22	SQ_Energy_9	0.000^	0.171		
23	SQ_Entropy_9	0.000^	0.098		
24	SQ_Homogeneity_9	0.000^	0.049		
25	SQ_Information_measure_of_correlation1_9	0.001^	0.270		
26	SQ_Information_measure_of_correlation2_9	0.000^	0.284		
27	SQ_Maximum_probability_9	0.000^	0.414		
28	SQ_Sum_entropy_9	0.901	0.458		
29	SQ_Sum_variance_9	0.000^	0.296		
30	SQ_Coarseness_9	0.002^	0.333	NGTDM	9x9 neighbourhood size
31	SQ_Cluster_prominence_9	0.325	0.778*	GLCM	9-pixel distance between the pixel of interest and its neighbour
32	SQ_Cluster_shade_9	0.068	0.124		
33	SQ_Range_all	0.002^	0.479	FOS	n/a
34	SQ_Sum_of_squares_variance_9	0.000^	0.059	GLCM	9-pixel distance between the pixel of interest and its neighbour

^Features ($n = 15$) showing statistically significant difference (p-value < 0.05) between *hardest-* and *easiest-to-interpret* normal cases of radiology trainees

[*] and highlighted in grey = important features ($n = 2$) from the machine learning classifier. The higher importance score means the more useful the features were for the classifier

Abbreviations: *FOS* first order statistics, *GLCM* gray-level co-occurrence matrix, *NGTDM* neighbourhood gray-tone difference matrix, *n/a* not applicable, *ROI* multiple regions of interests defined by the lattice-based approach covering the entire breast image, *SQ* largest square rectangular box inscribed within breast, *Std* standard deviation

of FOS. *Cluster prominence* measures the skewness and asymmetry of the GLCM [33] and was calculated using the squared-based approach [31]. *Range* describes the difference between maximum and minimum of image gray level values [25] and was calculated using the lattice-based method [30].

Figure 4 reveals that the difficulty of fatty or *low-density* normal cases does not significantly differ from that of dense or *high-density* cases (p-value = 0.12), with *low-density* cases appearing to be more challenging for RTs, albeit non-significant.

Discussion

In this proof-of-concept study, we explored (1) if using a set of global handcrafted radiomic or computer-extracted image features derived from mammograms, *hardest-* vs *easiest-to-interpret* normal cancer-free cases of RTs can be classified, and (2) whether any of these features are useful in this classification task.

Previous works [4, 5] recognised the usefulness of local radiomic features in identifying missed mammographic masses and false positive location errors of RTs, obtaining

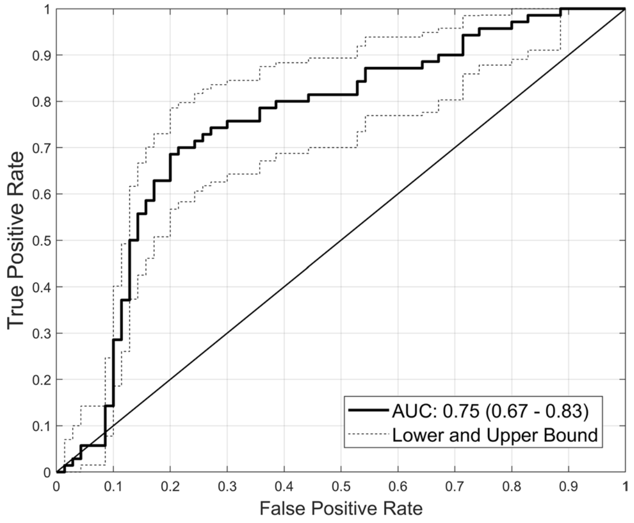

Fig. 2 Model performance. For discriminating *hardest-* from *easiest-to-interpret* normal cases of radiology trainees, AUC = 0.75 (95% confidence interval, 0.67– 0.83) was achieved by the random forest machine learning model

AUCs of up to 0.61 and accuracies of up to 40%. Other later studies [11, 16] indicated the value of GMRFs in predicting most *difficult-to-interpret* normal cases of general and experienced radiologists (over 20 years of experience reading mammograms), attaining AUCs of up to 0.73. Building on these recent research outputs [11, 16], we explored the feasibility of using GMRFs in describing RTs' *hardest-* vs *easiest-to-interpret* normal cases based on the hypothesis that the image characteristics of these two categories' cases are diverse. In addition, the results from our machine learning classifier revealed similar findings in that GMRFs (describing the whole image and largest square rectangular inscribed within breast) had the ability to distinguish between *hardest-* from *easiest-to-interpret* normal cases of RTs, achieving an AUC of 0.75 (95% CI, 0.67–0.83) (Fig. 2). This finding affirms the importance of GMRFs in predicting *hardest-to-interpret* normal cases for less-experience readers like RTs (Table 1).

Mammographic breast density using BI-RADS category are often employed as a surrogate measure in assessing difficult normal cases for RTs, where cases with higher density are regularly considered to be more difficult to interpret [17, 38]. However, studies have shown that breast density category details alone may not be completely reliable for predicting difficult/easy normal cases of radiologists including RTs [11, 39]. In line with these findings, the results from our dataset confirmed that BI-RADS density categories were not strongly correlated with difficulty scores (Fig. 4). Our GMRFs (e.g. *SQ_Cluster_prominence_9* and *ROI_Std_Range_all*) relating to *hardest-to-interpret* normal cases of RTs therefore may be used to provide supplementary clinical image information (in addition to BI-RADS breast density class) about most difficult features that RTs are likely to commit a false positive error. Also, since RTs find recognising normal image features challenging [13, 14], our findings could therefore aid their screening mammographic interpretation expertise development in recognising hardest and easiest breast features of normal cases which could then facilitate automatic hardest and easiest normal cases test set curation for customised education/training programmes.

Fig. 3 Scree plot showing significant global mammographic radiomic features. From 34 features, two important features were identified, indicating in the scree plot with the steep slope occurred after the second highest features (as shown by the red arrow). Those important features, ranked from the highest to the lowest important scores, were: (1) *SQ_Cluster_prominence_9* (feature# 31) of GLCM, and (2) *ROI_Std_Range_all* (feature# 16) of FOS. FOS first order statistics, GLCM gray-level co-occurrence matrix, ROI multiple regions of interests defined by the lattice-based approach covering the entire breast image, SQ largest square rectangular box inscribed within breast

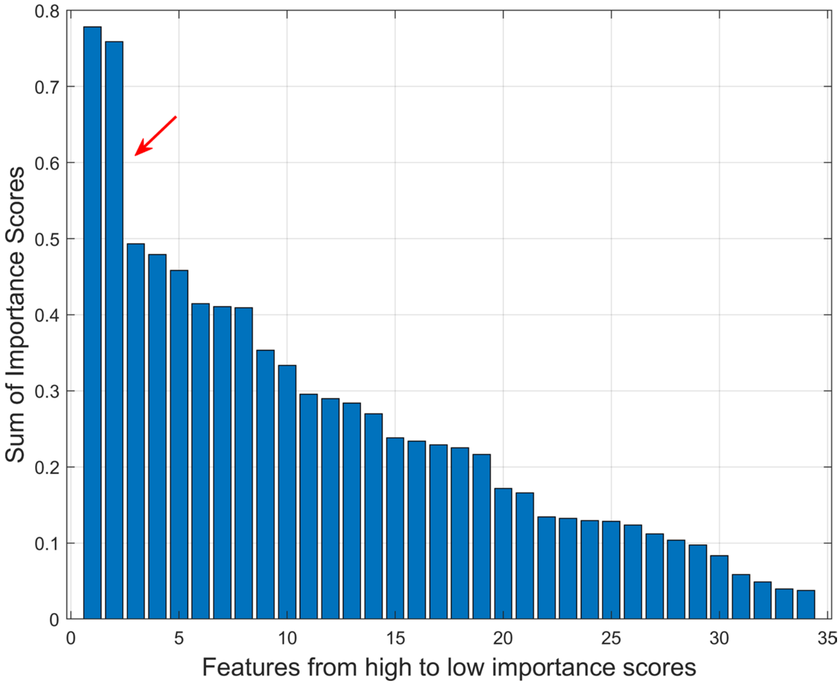

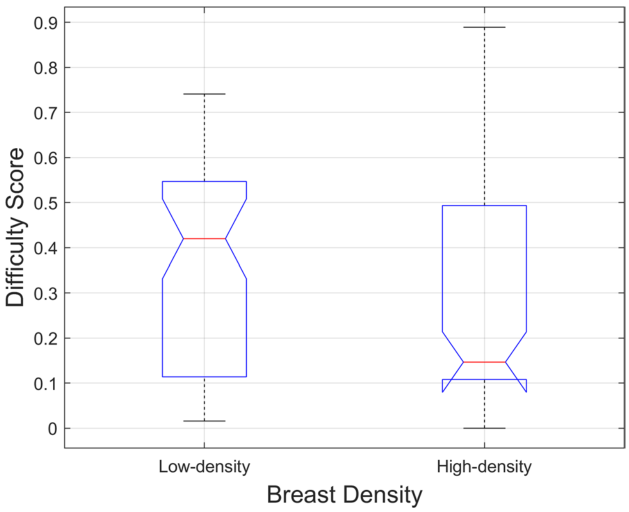

Fig. 4 Breast density comparison. Non statistically significant difference ($p = 0.12$) in the difficulty level was found between *low-density* and *high-density* normal cases of radiology trainees

Using the proposed model, we can create customised test sets tailored to the specific learning needs of trainees at different stages of their careers. For example, early-stage trainees could be presented with easier cases to build foundational skills, while more advanced trainees could be challenged with harder cases that reflect real-world complexities. This customised test set curation would allow for targeted education and training programmes that align with the trainees' current skill levels, helping them to progress more effectively through their learning journey.

Interestingly, when comparing two groups based on a single GMRF, 15 out of 34 features showed a statistically significant difference between *hardest-* and *easiest-to-interpret* normal cases of RTs ($p < 0.05$). However, when examining the 34 features together through our machine learning classifier, only two features (*cluster prominence*, i.e. *SQ_Cluster_prominence_9*, calculated using the squared-based approach [31] and *range*, i.e. *ROI_Std_Range_all*, calculated using the lattice-based method [30]) were found to be most useful in describing RTs' *hardest-* from *easiest-to-interpret* normal cases (Table 2 and Fig. 3). *Range*, in particular, has also been discovered to be a valuable feature in previous studies [11, 20] highlighting the significance of *range* in various classification tasks among different groups of readers (e.g. categorising *hardest-* from *easiest-to-interpret* normal cases of readers in general as well as RTs). While *cluster prominence* was not found to be an important feature in the previous work [11, 20], in this dataset, we observed that more difficult cases, which resulted in false positive errors more frequently, exhibited higher *cluster prominence* which is a measure of the skewness and asymmetry of the GLCM. This suggests that *cluster prominence* may be an important marker of highly challenging cases for RTs. A higher value of *cluster prominence* implies more asymmetry about the mean in the GLCM, while a lower value indicates a peak near the mean value and less variation about the mean. Intuitively, *cluster prominence* refers to the extent to which clusters of pixels within an image stand out from their surroundings. In other words, it measures the distinctiveness of clusters within the image with a higher *cluster prominence* value indicating that clusters are more salient or prominent within the image. In the context of our study, normal cases with higher *cluster prominence* value pose greater difficulty for trainees. Trainees may struggle with these cases because the heightened prominence of clusters within the image makes it more challenging to distinguish between normal tissue and potential abnormalities, resulting in false positive annotations. Although the features may be abstract in nature and not quantifiable by humans, they could be quantitatively measured using our radiomics approach and used as educational tools to teach and/or alert RTs that the higher the value of *cluster prominence*, the harder the case could be for RTs, increasing the chance of them making a false positive error. Furthermore, creating an alert system based on these features and educating RTs about the correlations between higher value of *cluster prominence* and harder cases can improve their ability to recognise difficult normal cases and enhance decision-making in clinical practice. Nonetheless, more studies are needed to further examine the effectiveness and reliability of these features.

This study also has a few limitations that should be recognised. It was a proof-of-concept study examining the efficacy of 34 handcrafted GMRFs [11] in identifying the *hardest-* from *easiest-to-interpret* confirmed cancer-free normal cases of 137 RTs (mostly with less than 1 year of experience reading mammograms) specifically. Only normal cases were included in the study which contained only those that had difficulty scores of greater than or equal to the 75th percentile (*hardest-to-interpret*) and less than or equal to the 25th percentile (*easiest-to-interpret*). LOOCV approach [36] was used to train and validate the model in order to maximise the use of the available data. The GMRFs were extracted from the region of interest delineated using the lattice-based [30] and squared-based [31] approaches. Future research should explore other approaches of identifying region of interest (e.g. retroareolar region), validating the model (e.g. hold-out method [36]), employing other difficult normal cases with difficulty scores falling outside the included range (e.g. scores that are less than the 75th percentile and greater than 25th percentile), and radiomic analysis involving local and/or deep learning features [26, 40].

Conclusions

In conclusion, in addition to previous research [11, 20], our work highlights the importance of GMRFs for classifying *hardest-* from *easiest-to-interpret* normal cases of RTs with two important features (c*luster prominence* and *range*) being identified. Our findings could be useful for developing RTs' interpretation expertise in identifying the most difficult image features of normal breast cases as well as enabling automatic and tailored test set curation of the most difficult cases for RTs' education/training programmes.

Acknowledgements The authors would like to express appreciation to the BreastScreen Reader Assessment Strategy (BREAST) programme at the University of Sydney for access and use of the data. BREAST is funded/supported by the Commonwealth Government Department of Health and Aged Care and the National Breast Cancer Foundation (NBCF), with their images provided by BreastScreen Australia and the Cancer Institute New South Wales (CINSW). The authors also would like to acknowledge the funding support for this research provided by the National Health and Medical Research Council [grant ID: APP1162872] and NBCF [grant ID: IIRS-18-089]. Z.G. is supported by the CINSW Early Career Fellowship [grant ID: 2022/ECF1426]. The authors wish to thank Dr Robert Heard for his statistical advice and the reviewers for their rigorous assessment of this manuscript.

Author Contribution All authors contributed to the study concept and design. Material preparation and data collection and analysis were performed by Somphone Siviengphanom and Ziba Gandomkar. The first draft of the manuscript was written by Somphone Siviengphanom, and all authors commented on previous versions of the manuscript. All authors read and approved the final manuscript.

Funding Open Access funding enabled and organized by CAUL and its Member Institutions. This work was supported by the National Health and Medical Research Council [grant ID: APP1162872] and National Breast Cancer Foundation [grant ID: IIRS-18–089] and Cancer Institute New South Wales [grant ID: 2022/ECF1426]. The funders played no role in study design, data collection and analysis, and interpretation of data, or the writing of this article.

Data Availability The data that support the findings of this study are available from BREAST, but restrictions apply to their availability, as they were used under license for the current study and are not publicly available. However, data may be available from the authors upon reasonable request and with permission from BREAST.

Declarations

Ethics Approval Ethical approval was obtained for this retrospective study from the Human Research Ethics Committee of the University of Sydney [Protocol number 2019/013 and 2017/028].

Consent to Participate Informed consent was obtained from all individual readers included in the study.

Consent for Publication Informed consent was obtained from all individual readers included in the study.

Conflict of Interest P.C.B. and Z.G. as well as an academic at the University of Sydney are CEO and Co-founder (P.C.B.)/employee (Z.G.) of DetectED-X, a company which aims to educate radiologists. The paper will not impact on DetectED-X's activities. All other authors of this manuscript, other than being employee of Western Sydney University (S.J.L.), employee (P.D.T.)/student (S.S.) of the University of Sydney, employee of the University of Technology Sydney (S.S.), declare no relationships with any companies, whose products or services may be related to the subject matter of the article.

References

1. Sung H, et al.: Global Cancer Statistics 2020: GLOBOCAN Estimates of Incidence and Mortality Worldwide for 36 Cancers in 185 Countries. CA: A Cancer Journal for Clinicians 71:209–249, 2021
2. Paci E: Summary of the Evidence of Breast Cancer Service Screening Outcomes in Europe and First Estimate of the Benefit and Harm Balance Sheet. Journal of Medical Screening 19:5-13, 2012
3. Ekpo EU, Alakhras M, Brennan P: Errors in Mammography Cannot be Solved Through Technology Alone. Asian Pac J Cancer Prev 19:291-301, 2018
4. Zhang J, Lo JY, Kuzmiak CM, Ghate SV, Yoon SC, Mazurowski MA: Using computer-extracted image features for modeling of error-making patterns in detection of mammographic masses among radiology residents. Medical Physics 41:091907, 2014
5. Zhang J, Silber JI, Mazurowski MA: Modeling false positive error making patterns in radiology trainees for improved mammography education. Journal of Biomedical Informatics 54:50-57, 2015
6. Wong DJ, et al.: Do reader characteristics affect diagnostic efficacy in screening mammography? A systematic review. Clinical Breast Cancer, 2023
7. Gandomkar Z, Lewis SJ, Li T, Ekpo EU, Brennan PC: A machine learning model based on readers' characteristics to predict their performances in reading screening mammograms. Breast Cancer 29:589-598, 2022
8. Hofvind S, et al.: Audit feedback on reading performance of screening mammograms: An international comparison. Journal of Medical Screening 23:150-159, 2016
9. Suleiman ME, Rickard M, Brennan PC: Perfecting detection through education. Radiography 26:S49-S53, 2020
10. Lee W, Peters G: Mammographic screening for breast cancer: A review. Journal of Medical Radiation Sciences 60:35-39, 2013
11. Siviengphanom S, Gandomkar Z, Lewis SJ, Brennan PC: Global radiomic features from mammography for predicting difficult-to-interpret normal cases. Journal of Digital Imaging 36:1541–1552, 2023
12. Vlahiotis A, Griffin B, Stavros Md FAT, Margolis J: Analysis of utilization patterns and associated costs of the breast imaging and diagnostic procedures after screening mammography. ClinicoEconomics and Outcomes Research Volume 10:157-167, 2018

13. Gandomkar Z, Mello-Thoms C: Visual search in breast imaging. Br J Radiol 92:20190057, 2019
14. Nodine CF, et al.: How experience and training influence mammography expertise. Acad Radiol 6:575-585, 1999
15. Buist DS, et al.: Influence of annual interpretive volume on screening mammography performance in the United States. Radiology 259:72-84, 2011
16. Siviengphanom S, Gandomkar Z, Lewis SJ, Brennan PC: Global mammographic radiomic signature can predict radiologists' difficult-to-interpret normal cases. Proc. SPIE Medical Imaging 2023: Image Perception, Observer Performance, and Technology Assessment: City
17. Ang ZZ, Rawashdeh MA, Heard R, Brennan PC, Lee W, Lewis SJ: Classification of normal screening mammograms is strongly influenced by perceived mammographic breast density. Journal of Medical Imaging and Radiation Oncology 61:461-469, 2017
18. Darker I, Chen Y, Gale A: Health professionals' agreement on density judgements and successful abnormality identification within the UK Breast Screening Programme. Proc. SPIE Medical Imaging: City
19. Gandomkar Z, et al.: Reliability of radiologists' first impression when interpreting a screening mammogram. PLOS ONE 18:1-19, 2023
20. Siviengphanom S, Lewis SJ, Brennan PC, Gandomkar Z: Computer-extracted global radiomic features can predict the radiologists' first impression about the abnormality of a screening mammogram. British Journal of Radiology 97:168–179, 2024
21. Brennan PC, et al.: Radiologists can detect the 'gist' of breast cancer before any overt signs of cancer appear. Sci Rep 8:1-12, 2018
22. Gandomkar Z, et al.: Global processing provides malignancy evidence complementary to the information captured by humans or machines following detailed mammogram inspection. Sci Rep 11:1-12, 2021
23. Siviengphanom S, Lewis SJ, Brennan PC, Gandomkar Z: Predicting the gist of breast cancer on a screening mammogram using global radiomic features. Proc. SPIE Medical Imaging 2024: Image Perception, Observer Performance, and Technology Assessment: City
24. Evans KK, Georgian-Smith D, Tambouret R, Birdwell RL, Wolfe JM: The gist of the abnormal: Above-chance medical decision making in the blink of an eye. Psychonomic Bulletin & Review 20:1170-1175, 2013
25. Gillies RJ, Kinahan PE, Hricak H: Radiomics: Images Are More than Pictures, They Are Data. Radiology 278:563-577, 2016
26. Siviengphanom S, Gandomkar Z, Lewis SJ, Brennan PC: Mammography-based Radiomics in Breast Cancer: A Scoping Review of Current Knowledge and Future Needs. Academic Radiology 29:1228-1247, 2021
27. Gandomkar Z, et al.: An end-to-end deep learning model can detect the gist of the abnormal in prior mammograms as perceived by experienced radiologists. Proc. SPIE Medical Imaging 2021: Image Perception, Observer Performance, and Technology Assessment: City
28. Brennan P, Lee W, Tapia K: Breast Screen Reader Assessment Strategy (BREAST): A Research Infrastructure with a Translational Objective, Cambridge: Cambridge University Press, 2018
29. McEntee M, Brennan P, Evanoff M, Phillps P, O Connor W, Manning D: Optimum ambient lighting conditions for the viewing of softcopy radiological images: SPIE, 2006
30. Zheng Y, et al.: Parenchymal texture analysis in digital mammography: A fully automated pipeline for breast cancer risk assessment. Medical Physics 42:4149-4160, 2015
31. Gandomkar Z, Suleiman M, Demchig D, Brennan P, McEntee M: BI-RADS density categorization using deep neural networks. Proc. SPIE 10952, Medical Imaging 2019: Image Perception, Observer Performance, and Technology Assessment: City
32. Haga A, et al.: Standardization of imaging features for radiomics analysis. The Journal of Medical Investigation 66:35-37, 2019
33. Haralick RM, Shanmugam K, Dinstein IH: Textural Features for Image Classification. IEEE Transactions on Systems, Man, and Cybernetics SMC-3:610–621, 1973
34. Amadasun M, King R: Textural features corresponding to textural properties. IEEE Transactions on Systems, Man, and Cybernetics 19:1264-1274, 1989
35. Breiman L: Random Forests. Machine Learning 45:5-32, 2001
36. Molinaro AM, Simon R, Pfeiffer RM: Prediction error estimation: a comparison of resampling methods. Bioinformatics 21:3301-3307, 2005
37. Ledesma RD, Valero-Mora P, Macbeth G: The Scree Test and the Number of Factors: a Dynamic Graphics Approach. The Spanish Journal of Psychology 18, 2015
38. A Tapia K, Rickard MT, McEntee MF, Garvey G, Lydiard L, C Brennan P: Impact of breast density on cancer detection: observations from digital mammography test sets. International Journal of Radiology & Radiation Therapy 7:36–41, 2020
39. Grimm LJ, Kuzmiak CM, Ghate SV, Yoon SC, Mazurowski MA: Radiology Resident Mammography Training. Academic Radiology 21:888-892, 2014
40. Pertuz S, Torres GF, Tamimi R, Kamarainen J: Open Framework for Mammography-based Breast Cancer Risk Assessment. Proc. 2019 IEEE EMBS International Conference on Biomedical & Health Informatics (BHI): City